Cardio-Vascular BeatDown (CBD)

Aisling Power, Nathan Hodges and Oliver Pernie

May 4, 2017

Abstract

This paper highlights the use of Hodgkin-Huxley type models to analyze the action potential across three types of cardiac cells: sino-atrial, purkinje fibers and ventricular myocytes. The main idea with Hodgkin-Huxley type models is that it is possible to capture the dynamics of action potential generation by treating the ionic currents that flow across cell membranes as a closed electrical circuit. The ionic currents involved in action potential generation vary with each cell; The shape of the action potential also varies, which reflects the function that the cell has in the cardiac system. The cells under consideration fall into two categories: pacemaker cells and cardiac muscle cells. This work investigates the dynamics of these cells and associated ionic currents to better understand how their action potential relate to their function in the heart as well as to understand the differences and similarities between the action potentials of different types of cardiac cells.

1 Introduction

The Hodgkin-Huxley (HH) model was developed in 1952 to represent the dynamics of action potentials in neurons. The model was developed by fitting ordinary differential equations to data from voltage clamp experiments of the neurons in squid. This proved to be successful in understanding the dynamics of their electro-physiology, and subsequent models based on the principles of the HH model were developed for other electro-physical systems. Using this, insight can be gained regarding the inner workings of other electrical systems in the heart and of cardiac phenomenon.

Action potentials (AP) are periodic electrical excitations that are induced by ion gradients between membranes. Models of AP also show how ion concentrations change over time. There are four main types of cardiac cells that produce AP: nodal cells (sino-atrial (SA) and atrioventricular (AV) nodes), Purkinje fiber cells, Atrial cells, and Myocardial cells, each found in separate locations of the heart.

The AP produced in cells is determined by ion channels in the cell membrane. They act as gatekeepers by regulating the inward and outward flow of ions based on the voltages within the cell. Each channel is described using gating variables that govern the flow of each ion so as to increase (depolarize) or decrease (re-polarize) the membrane potential. The AP shape differs for each type of cardiac cell. The cardiac cells that are modeled in this paper are the SA nodal cells, Purkinje fiber cells, and ventricular myocardial cells.

SA nodal cells are located in the right atrium and spontaneously produce APs that act as a signal to other cells, inducing contractions of the heart[5]. The SA nodal cells act as the pacemaker and so have no resting potential. Instead of resting before another AP is produced, there is an automatic depolarization after each AP. This is called the pacemaker potential and it is primarily governed by sodium, calcium and potassium currents.

Purkinje fiber cells are located in the inner ventricular walls of the heart. Purkinje fibers conduct AP more quickly and efficiently than other cells in the heart[4] and are primarily for fast conduction[1]. These fibers also allow for synchronized ventricle contraction and are very important in maintaining consistent heart rhythms. The Purkinje fibers and ventricular myocardial cells have longer AP than the SA nodal cells and help facilitate and control muscle contraction[1].

Ventricular myocytes are prevalent throughout the ventricles and are the striated muscle cells responsible for the contraction of the heart tissue. They require an applied current from neighboring cells to generate an

AP that induces an influx of calcium needed to operate the t-tubles that pull the walls of the cell membrane together.[8] These cells are connected via gap junctions and the collective contraction of each cell pushes blood out of the heart.

There are five phases[6] of cardiac action potential and all cells follow a similar framework. The different phases with respect to the action potential can be seen in figure 1. This figure is of a specific cell type but can be used for general purposes.
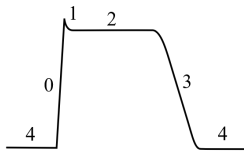

Figure 1: Phases of Action Potentials. See [7]

i. Phase 0 is the depolarization phase. In non-pacemaker cells, when the membrane potential reaches a certain threshold value, usually through an external stimulus, the sodium channels open and floods the cell with positive ions, increasing the potential. This creates the initial spike in the AP. The slope of phase 0 determines the speed of depolarization and corresponds to the conduction velocity. In pacemaker cells, the initial increase in voltage is due to L-type calcium channels that activate slower than sodium channels, and thus the SA nodal AP has a smaller slope than other cell's AP.

ii. Phase 1 is a rapid inactivation of voltage gated sodium channels and a fluctuation in the activity of potassium channels. Phase 1 is not present in pacemaker cells.

iii. Phase 2 is the "plateau" phase; The membrane potential remains relatively constant until the membrane repolarizes. At this point, potassium flows out of the cell and calcium flows into the cell, creating an equilibrium. This phase causes the heart's APs to be of longer durations, thereby helping to prevent irregular heartbeats. Phase 2 does not happen in pacemaker cells.

iv. Phase 3 is the rapid repolarization phase. This is characterized by the calcium channels closing while the potassium channel's are left open. Once repolarization is complete, the cell can respond to new stimulus to produce another AP.

v. Stage 4 is when there is no or little flow of ions across the cell membrane and the cell is at resting membrane potential. For pacemaker cells, phase 4 is when the cells are at their pacemaker potential although this phase lasts for a short period of time and is characterized with a slow increase in potential.

This work analyzes and investigates the ion currents and ion channels that contribute to the production of APs in three different cells. The models in consideration are the Nobel model, proposed in 1962 for Purkinje fiber cell APs, the Yanagihara-Noma-Irisawa(YNI) model, proposed in 1980 to model SA nodal cells, and the Beeler-Reuter model, proposed in 1977 to model ventricular myocardial cells.

2 Methods

The models analyzed use the HH framework but incorporate alternative ions and currents. Each model consists of a system of nonlinear, ordinary differential equations, solved in the R program. Subsequent analysis' and graphs were also done in R. The general form for an AP of a given system is

$$\frac{dV}{dt} = (I_{applied} - I_{ion})/C_m.$$

C_m is the capacitance of the cell membrane and has units of $\mu F/cm^2$. I_{ion} consists of the ionic currents prevalent in the cell. All of the currents are in units $\mu A/cm^2$. The ionic currents themselves are governed by gating variables that represent the probabilities of a gate being open or not. They are dimensionless and are in the form

$$\frac{dw}{dt} = \alpha_w(1 - w) - \beta_w w, \tag{1}$$

where w corresponds to a chosen gate. α_w and $beta_w$ are rate constants of the transition between the opened and closed states of the gates; They are given by:

$$\frac{c_1 e^{\frac{V - V_0}{c_2}} + c_3(V - V_0)}{1 + c_4 e^{\frac{V - V_0}{5}}}. \tag{2}$$

The general equation for the steady state values of the gating variables is

$$w_\infty = \frac{\alpha_w}{\alpha_w + \beta_w}. \tag{3}$$

The general equation for time constant of a gating variable is given by

$$\tau_w = \frac{1}{\alpha_w + \beta_w}. \tag{4}$$

Purkinje Fiber Cells

i. The Nobel model assumes 3 ionic currents; an inward sodium current, an instantaneous, voltage-dependent potassium current(K_2), and a time-dependent potassium current(K_1). Applying Kirchoff's Law we get

$$0 = C_m \frac{dV}{dt} + I_{eq} + I_{Na} + I_{K_1} + I_{K_2} - I_{app}.$$

Our currents are subsequently given by

$$I = g * (V - V_0),$$

where g is the associated ion conductance and V_0 is the associated ion equilibrium potential. In the Noble model, $C_m = 12$, which is unreasonably high despite producing the most accurate results. Formulas for each ion's conductance is given below.

$g_{eq} = 0$
$g_{K_2} = 1.2n^4$
$g_{K_1} = 1/2e^{-\frac{V+90}{50}}$
$g_{Na} = 400m^3h + g_i$

g_i provides a constant inward sodium current that, along with the high capacitance, enables prolonged action potentials; m, n, and h are the time dependent gating channel variables for the membrane. Unless specified otherwise, the gating variables take the form of equation 1, where $w = m, n, h$, and α_w and β_w take the form of equation 2. The constants, developed from data, are given by:

	c_1	c_2	c_3	c_4	c_5	V_0
α_m	0	–	0.1	-1	-15	-48
β_m	0	–	-0.12	-1	5	-8
α_h	0.17	-20	0	0	–	-90
β_h	1	∞	0	1	-10	-42
α_n	0	–	0.00001	-1	-10	-50
β_n	0.002	-80	0	0	–	-90

Ventricular Cells

i. The Beeler and Reuter model incorporated the flux of calcium ions across the membrane the conservation of current is summarized as follows,

$$\frac{dV}{dt} = -\frac{1}{C_m}(I_{Na} + I_k + I_s + I_x - I_{app}).$$

The initial sodium current responsible for phase 0 depolarization is

$$I_{Na} = (4m^3hj + 0.003)(V - 50),$$

with j being introduced as a reactivation variable. The potassium current has a time independent current and a time activated outward current, similar to the Noble model.

$$I_k = 1.4\frac{e^{0.04(V+85)} - 1}{e^{0.08(V+53)} + e^{0.04(V+53)}} + 0.07\frac{V + 23}{1 - e^{-0.04(V+23)}},$$

$$I_x = 0.8x\frac{e^{0.04(V+77)} - 1}{e^{0.04(V+35)}}.$$

One of the main differences between the purkinje fibers and ventricular cells is the importance of Ca^{2+} ions[1] that are responsible for the operation of the transverse tubular system. This slow current is

$$I_s = 0.09fd(V + 82.3 + 13.0287\ln([Ca]),$$

where $[Ca]^{2+}$ represents the concentration of calcium ions.

Below is the table of parameter values that were used throughout this study for the gating variables, equation 2 in the BR model.[1]

	c_1	c_2	c_3	c_4	c_5	V_0
α_m	0	−	1	−1	−10	−47
β_m	40	−17.86	0	0	−	−72
α_h	0.126	−4	0	0	−	−77
β_h	1.7	∞	0	1	−12.2	−22.5
α_j	0.055	−4	0	1	−5	−78
β_j	0.3	∞	0	1	−10	−32
α_d	0.095	−100	0	1	−13.9	5
β_d	0.07	−58.5	0	1	20	−44
α_f	0.12	−125	0	1	6.67	−28
β_f	0.0065	−50	0	1	−5	−30
α_x	0.0005	12	0	1	17.5	−50
β_x	0.0013	−16.67	0	1	−25	−20

Sino-atrial Nodal Cells

i. The YNI model, for SA nodal cells, incorporates five currents and seven variable and is given by

$$\frac{dV}{dt} = (I_{applied} - (I_{Na} + I_s + I_h + I_l + I_K))/C_m.$$

4

I_{Na} is the sodium current, I_s is a slow inward current, I_h is the hyper-polarization current, I_l is the time dependent leak current, and I_K is the potassium current. The equation of these currents are, respectively,

$$I_{Na} = 0.5m^3 h(V - 30),$$

$$I_s = 12.5(0.95d + 0.05)(0.95f + 0.05)(e^{\frac{V-30}{15}} - 1),$$

$$I_h = 0.4q(V + 25), I_l = 0.8(1 - e^{-\frac{V+60}{20}}),$$

$$I_K = 0.7p\frac{e^{0.0277(V+90)-1)}}{e^{0.0277(V+40)}}.$$

The gating variables are in the same form as equation 1, and the αs and βs follow the form of equation 2 except for the following:

$$\alpha_p = (9 * 10^{-3})\frac{1}{1 + e^{-\frac{V+3.8}{9.71}}} + 6 * 10^{-4},$$

$$\alpha_q = (3.4 * 10^{-4})\frac{V + 100}{e^{\frac{V+100}{4.4}} - 1} + 4.95 * 10^{-5},$$

$$\beta_q = (5 * 10^{-2})\frac{V + 35}{1 - e^{-\frac{V+40}{6}}} + 8.45 * 10^{-5},$$

$$\alpha_d = (1.045 * 10^{-2})\frac{V + 35}{1 - e^{-\frac{V+35}{2.5}}} + 3.125 * 10^{-2}\frac{V}{1 - e^{-\frac{V}{4.8}}},$$

$$\beta_f = (9.44 * 10^{-4})\frac{V + 60}{1 + e^{-\frac{V+29.5}{4.16}}}.$$

The constants for the YNI model in equation 1 are

	c_1	c_2	c_3	c_4	c_5	V_0
α_m	0	—	1	−1	−10	−37
β_m	40	−17.8	0	0	—	−62
α_h	1209	−6.534	0	0	—	−20
β_h	1	∞	0	1	−10	−30
α_p	0	—	−0.000225	−1	13.3	−40
β_d	0	—	−0.00421	−1	2.5	5
α_f	0	—	−0.000355	−1	5.633	−20

3   Results

The Noble Model

i. The plot below shows action potentials for various applied currents. The initial upstroke is due to a large inward Na^+ current. This current continues produces the plateau of membrane potential after the initial upstroke.
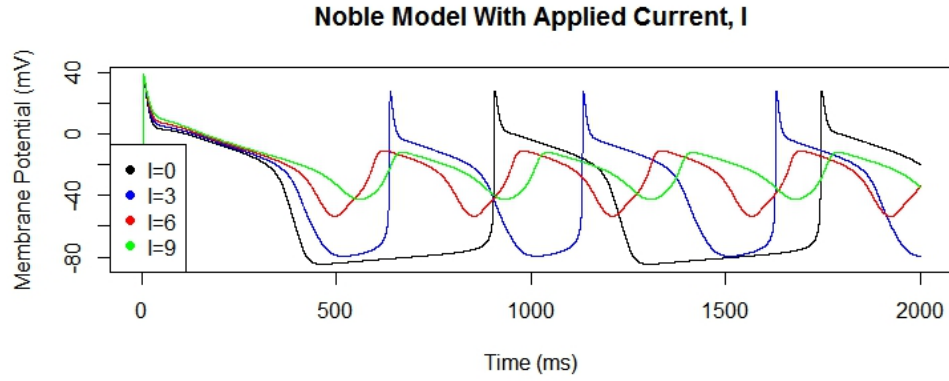
Figure 2: Action potentials for the Purkinje fiber cells with varied applied currents.

As the applied current is increased, the refractory period of the cell decreases and the membrane potential doesnt decrease enough to allow the oncoming influx of Na^+ ions to produce an AP.

ii. Figure 3 shows the ion currents of the Purkinje fiber cell action potential where $I_{app} = 0$ as they change in time. This includes the sodium ion current and both the time-dependent(K_1) and instantaneous potassium currents(K_2). Beneath that are the gating variable probabilities, allowing one to associate the m and h gates with sodium, and the n-gate with K_2.
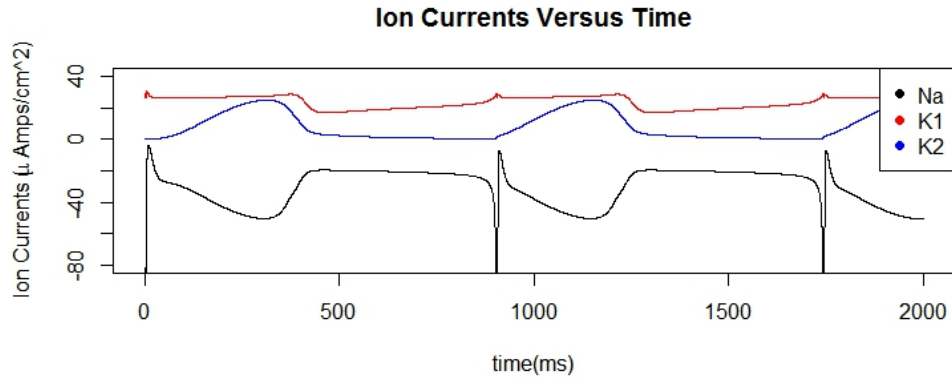
Figure 3: Sodium and potassium currents vs. time for the Purkinje fiber cell

6
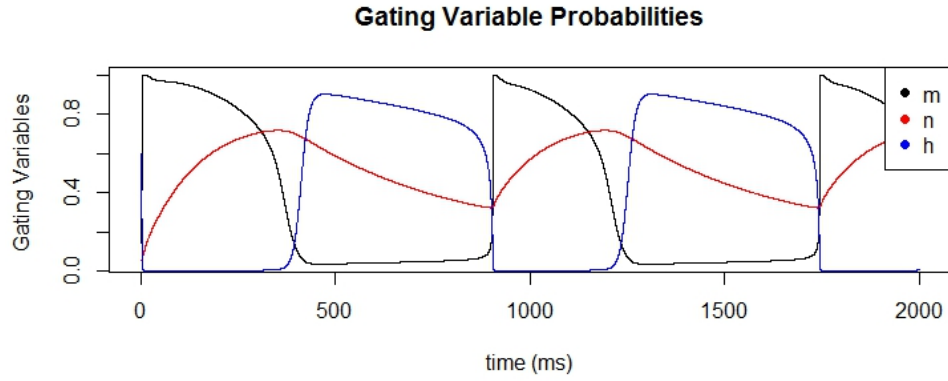
Figure 4: Phases of Action Potentials

The refractory period is characterized by a steady current of potassium ions into the cell after the influx of Na^+ ions. This slowly reduces the overall membrane potential, prepping the cell for another AP. Although producing an accurate qualitative model, the Noble Model is physiologically inept. Particularly in that it ignores a calcium ion current, which data has shown to be the cause of the plateau in AP. Note that the quick initial sodium current activates, goes to zero, and then continues through the plateau phase of the AP. This shows how the Noble model uses sodium ions, rather than calcium ions, to produce this phenomenon.

The Beeler-Reuter model (BR) Model

i. The AP for the BR model, similar to that of the purkinje fibers, is plotted below in figure 5 for various applied currents. Units are in μA. As you can see, larger currents imply longer plateau periods and a larger resting potential.
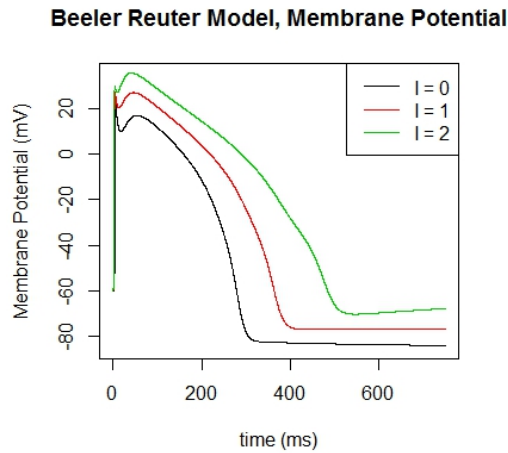

Figure 5: Action Potentials for Beeler-Reuter model.

7

ii. Figure 6 is a plot of the gating variables that indicate activation and deactivation of ionic currents which are shown in figure 7. Notice in figure 7 that negative currents indicate a flux of ions into the cell. The initial influx of sodium from I_{Na} is very large, but finite and has been cropped to show the other currents. For example the outward potassium current I_x is gated with x and contributes no current across the membrane, then gradually it reaches its maximum at approximately 300ms before tapering out to 0 at larger times.
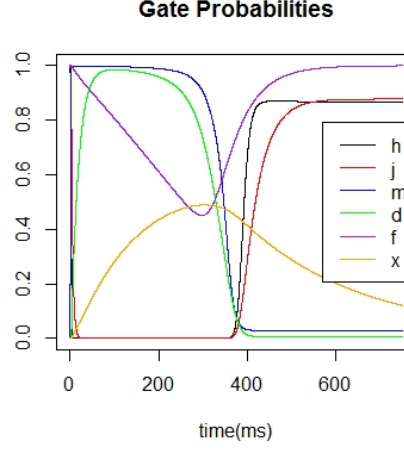
Gate Probabilities

Figure 6: Probability that a gate is open during AP.

I_k corresponds to a continuous outward flow of sodium, similar to currents used in the Noble model, and is the only current that does not correspond to the activation of any gate. Gates f and d correspond to current I_s, which governs the flow of calcium. From the value of these variables over time one can see that calcium ions enter the cell most rapidly after phase 1 falls off rapidly at the end of the AP.
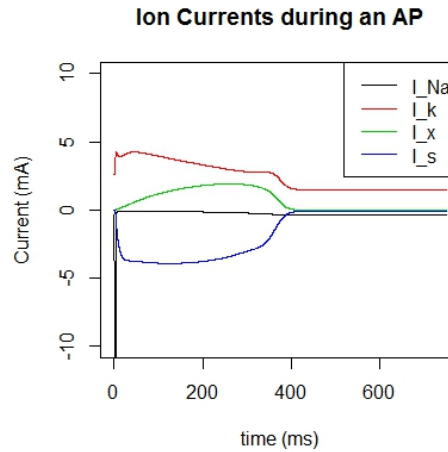
Ion Currents during an AP

Figure 7: Ionic currents during AP of BR model.

iii. Below is a plot of the calcium concentration within the cell through an AP. The concentration was assumed satisfy the differential equation,

$$\frac{d[Ca]}{dt} = 0.07(10^{-7} - c) - 10^{-7}I_s.$$

All though the BR model was successful in simulating the inter cellular calcium concentration it failed to capture the intensity of the initial sodium current. This data is available now and is incorporated into a more commonly used Luo-Rudy model for ventricular myocardial cells.
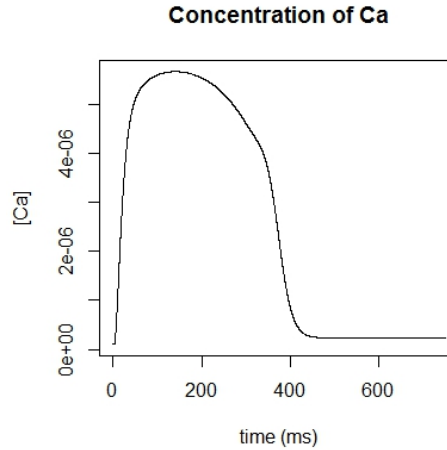

Figure 8: Concentration of Calcium ions in the cytosol.

The Yanagihara-Noma-Irisawa(YNI) Model

i. Figure 8 shows the APs produced by the SA node in a rabbit as predicted by the YNI model. There are three APs with various applied currents. The normal AP of an SA nodal cell, where $I = 0$, is given in black. The other currents show that any applied current will produce irregularities in the AP and a large enough current will stop APs. Unlike Purkinje fibers and ventricular cells, the SA nodal cells do not require a stimulus to produce an AP; thus the AP discontinues at relatively low applied currents.
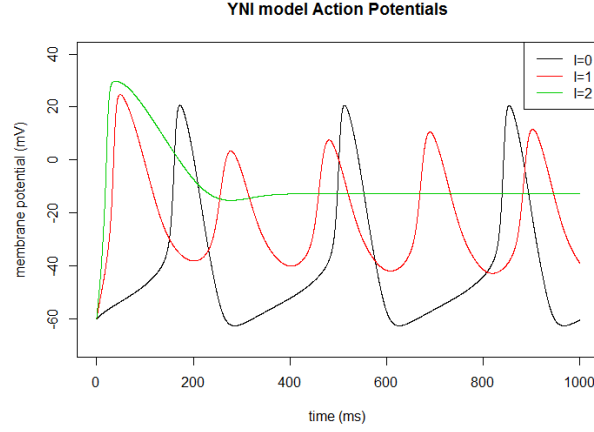
Figure 9: Action potentials for SA nodal cells with three different applied currents.

ii. Figure 9 shows the ion currents that contribute to the production of AP against time. There is no assumed constant applied current to elongate the duration of the AP. The slow inward ion current, I_s, contributes the most to negative voltages, whereas the K^+ and leak currents seem to contribute to higher voltages. The spike in I_s precipitates the rapid decrease in voltage that occurs around 150 ms.
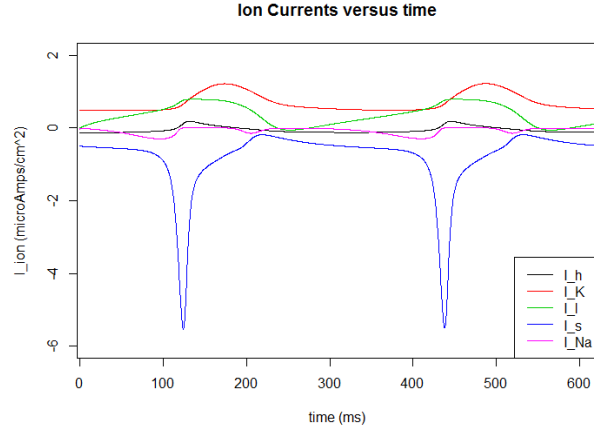

Figure 10: Ionic currents vs. time for the SA nodal cell

iii. Figure 10 shows steady state gate values against the membrane potential, the values are found using equation 3. This graph shows the behavior of each gate as the potential changes, providing insight to which gates increase or decrease voltage. It is clear from the graph that the f, h, and q gates are most likely to open at low voltages; whereas the m, d, and p gates are most likely to open at higher, more positive voltages.
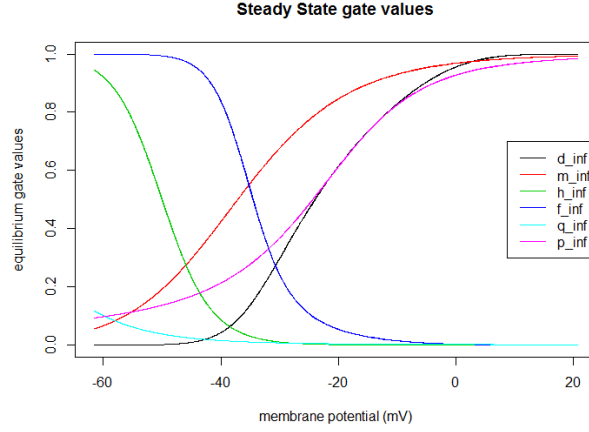
10

Figure 11: Gating variables at their steady state values versus membrane potential in the YNI model

iv. Figure 11 shows the probability of a gate being open as functions of time. They are the real time values of the gating variables as they change to produce AP. Figure 11 shows more complex behavior than figure 10 in that the gates open at differing times, dependent upon the behavior and phase of the AP that they correspond to.
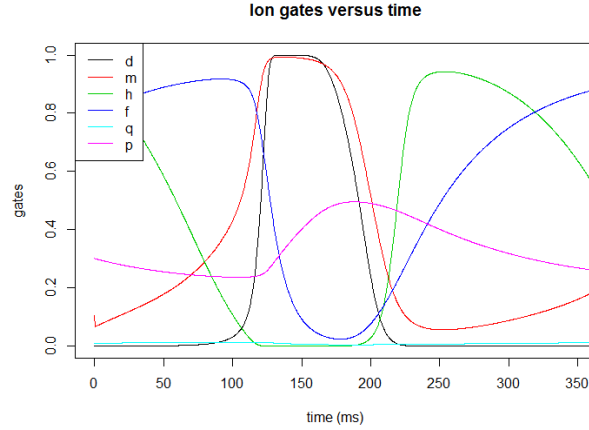

Figure 12: The probability of ionic gates being open as a function of time in the YNI model.

v. Figure 12 shows time constants for the gating variables as they change with potential, using equation 4. A short time constant corresponds to the gate approaching it's steady state potential quicker, whereas a large time constant corresponds to the gate approaching it's steady state potential slowly. p, q, and f have larger time constants as the potential increases, although they close when the potential turns positive, meaning that the gates approach equilibrium values increasingly quick at higher potentials. Figure 12 also shows that the h, m, and d gates always have small time constants, meaning they act and respond quickly to changes in potential.
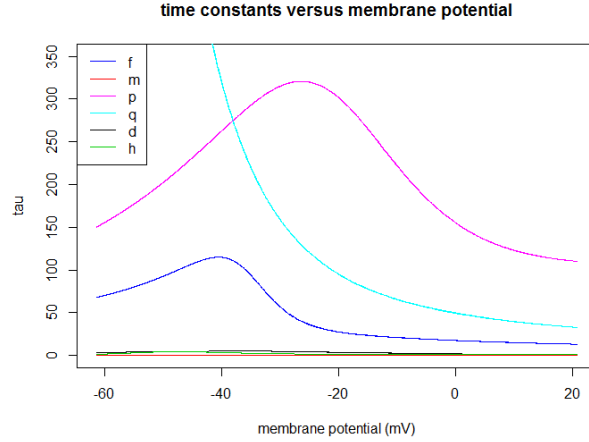
11

Figure 13: Time constants of gating variables versus membrane potential.

Analysis of figure 11 shows that the f, h, and q gates activate at lower potentials, and thus are inactivation gates. The m, d, and p gates activate at higher potentials, and thus are activation gates. The sodium currents relationship with these gates is given by the term m^3h, such that sodium will enter the cell slowly at low potentials and fast at high ones. This corresponds to the expected behavior of an AP as sodium influx is the main contributor to the initial spike and depolarization of an AP. The small time constants of the gates shown in figure 13 confirm their fast behavior in figures 11 and 12.

The slow inward I_s current is proportional to the d and f gates. Figure 12 shows that the d gate is the main contributor to the AP. f quickly repolarizes the cell after the initial spike. This is why there is no phase 2 of AP in SA nodal cells. Note that the point where the d and f gate values cross corresponds to negatives spike in I_s shown in figure 10.

The hyperpolarizing current I_h is related to the q gate. This current is a small contributor to the overall APs in figures 11 and 12. The probability that the q gate is open is higher at small voltages, but essentially zero once the potential reaches about -40 mV. Figure 8 shows the q gate approaches equilibrium very slowly at low potentials and faster as the voltage increases. This confirms that the gate is active at low voltages, since the equilibrium is close to zero.

The leak current is not dependent on gates; Only time and voltage and thus cannot be thoroughly analyzed in the context of this investigation.

The potassium current is represented with the p gate. Data has found that the p gate does not contribute to the initial rapid depolarization but activates just before the AP reaches its maximum and does not produce large currents. Figure 13 shows the time constant for the p gate is large, confirming that the gate acts slowly.

4   Discussion and Conclusion

Each model provides a useful framework for preliminary mathematical investigations into the dynamics of AP production. Modeling the flow of ions through a cell membrane as an electrical circuit is useful and accurate. The formation of each model utilizes this basic premise coupled with equations for ion currents that were developed via curve fitting data from voltage clamp experiments. Therefore, the formulas themselves have no physical meaning. The expected dynamics of the AP for each type of cell confirms their function.

The Noble Model of Purkinje Fiber cells, although the simplest, captures the dynamics of the heart's APs and showed that models of the HH type are valid when modeling heart cells. Essentially, the issue was modifying the HH model to account for prolonged duration of the AP during phase 2. It was observed that an assumed positive inward ion current, which activates after the initial upstroke of the AP, would cause this phenomenon. Thus the Noble model assumes an extra inward sodium current.

The Beeler-Reuter Model added more complexity to the Noble model by incorporating an inward calcium current. This makes the BR model more physiologically correct however the final form of a myocardial AP model has not been agreed upon. The next step for modeling muscle contraction would be to couple a network of myocardial cells via the cable equation to simulate the propagation of AP throughout the tissue.

Results from the analysis of the YNI model successfully illustrates the general behavior of SA nodal cells. The AP works best with no applied current as expected in pacemaker cells and the AP duration is regular with no constant resting potential. The pacemaker potential is about -60 mV and the associated graphs show that the threshold potential is about -40 mV. At this point other channels open to quickly move the cell into a higher potential. Physically, this corresponds to calcium channels opening although this model was developed before the discovery of calcium current and so does not include it.

Further studies could analyze more updated models as well as investigate the relationship between conductance and AP generation. Analyzing irregularities in AP using stability analysis is also useful as it could provide insight into the nature of cardiac arrhythmias.

References

[1] James Sneyd, James P. Keener, *Mathematical Physiology* Chapter 12. 2nd ed. : Springer, 2009.

[2] Zhenxing Pan, Rei Yamaguchi, Shinji Doi. 2011. Bifurcation analysis and effects of changing ionic conductances on pacemaker rhythm in a sinoatrial node cell model. *Biosystems* 106(1):9-18.

[3] Beata Jackowska-Zduniak and Urszula Forys. 2016. Mathematical model of the atrioventricular nodal double response tachycardia and double-fire pathology. *Mathematical Biosciences and Engineering* 13(6):1143-1158.

[4] Penelope A. Boyden, Masanori Birose, Wen Dun. 2010. Cardiac Purkinje cells. *Heart Rhythm* 7(1) : 127-135.

[5] M.R. Boyett, H, Honjo, and I. Kodama. 2000. The sinoatrial node, a heterogeneous pacemaker structure. *Cardiovascular Research* 47(4):658-687.

[6] Yelle, Dominqe, and Greg Ikonnikov. "Physiology of cardiac conduction and contractility." *McMaster Pathophysiology Review*. Web. 02 May 2017.

[7] "Cardiac action potential." Wikipedia. Wikimedia Foundation, 02 May 2017. Web. 04 May 2017.

[8] "The Structure and Function of the Cardiac Myocyte: A Review of Fundamental Concepts" Walker, C.Allyson et al. *The Journal of Thoracic and Cardiovascular Surgery* 118(2):375-382.